

Revisiting Residual Connections for Neural Structure Learning

Anonymous authors

Paper under double-blind review

Abstract

Recent studies reveal that deep representation learning models without proper regularization can suffer from the dimensional collapse issue, i.e., representation vectors span over a lower dimensional space. In the domain of graph deep representation learning, the phenomenon that the node representations are indistinguishable and even shrink to a constant vector is called oversmoothing. Based on the analysis of the rank of node representations, we find that representation oversmoothing and dimensional collapse are highly related to each other for deep graph neural networks (GNNs), and the oversmoothing problem can be interpreted by the dimensional collapse of the representation matrix. Then, to address the dimensional collapse and the triggered oversmoothing in deep graph neural networks, we first find vanilla residual connections and contrastive learning producing sub-optimal outcomes by ignoring the structural information of graph data. Motivated by this, we propose a novel graph neural network named GearGNN to address the oversmoothing issue from the perspective of addressing dimensional collapse in two folds. Specifically, in GearGNN, we design a topology-preserving residual connection for graph neural networks to force the low-rank of hidden representations close to the full-rank input features. Also, we propose the structure-guided contrastive loss to ensure only close neighbors who share similar local connections can have similar representations. Empirical experiments on multiple real-world datasets demonstrate that GearGNN outperforms state-of-the-art deep graph representation baseline algorithms.

1 Introduction

Representation learning models have achieved outstanding performance for various application domains by outputting informative hidden representations, such as computer vision and natural language processing. Recent studies (Hua et al., 2021; Jing et al., 2022; Guo et al., 2023) show that deep representation learning models without proper regularization tend to produce representations that collapse along certain directions, known as the *dimensional collapse*, which can be further interpreted by the visualization of the singularity ranking of the matrices of representations (Hua et al., 2021). In the era of big data, graph structures recently received increasing research attention for their ability to encode complex interactions. Similarly, the deep representation learning models on graphs are also found affected by representation issues, i.e., the node representation vectors outputted by deeper graph neural networks are not discriminative from each other and directly hurt the performance of node classification and link prediction tasks and their corresponding applications. This phenomenon is called *oversmoothing* in the graph representation learning domain (Li et al., 2018; Oono & Suzuki, 2020; Rusch et al., 2023).

In this paper, we first find that the oversmoothing in graph deep learning can be interpreted by dimensional collapse from the low-rank of representation matrix, a detailed theoretical derivation can be found in Appendix A. To empirically demonstrate that dimensional collapse exists in the graph representation learning domain, we conduct a toy experiment on the Cora (Lu & Getoor, 2003) benchmark dataset by exploring the rank of the covariance matrix of the node representations. The analysis is visualized in Figure 1, where the x -axis is the index of the sorted singular values of the covariance matrix of the representation matrix, and the y -axis is the logarithm of the singular value. In Figure 1, we can see that the number of non-zero singular values is much smaller than the number of dimensions for a GCN graph neural network (Kipf & Welling, 2017). It suggests that the representation matrix is *low-rank*, and the discrimination of node representation

vectors only relies on a few dimensions, which naturally increases the difficulty of effectively discriminating node presentations and makes tasks like node classification and link prediction groundless.

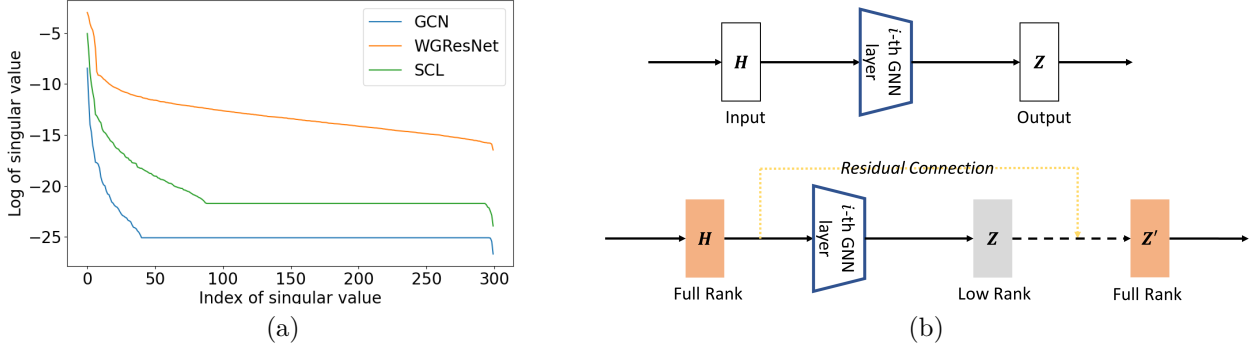


Figure 1: (a). A toy example on the Cora dataset to demonstrate the rank deficiency, where GCN is chosen as the backbone, the number of layers is set to 64 and the dimension of representation is 100. (b). The visualization about how vanilla residual connections of neural layers turn the low-rank representation Z into a full-rank representation Z' .

To address the dimensional collapse problem in deep neural networks, residual connections (He et al., 2016) among neural layers can be an effective manner, i.e., it has been discovered that residual connections across neural network layers force the low-rank of hidden representations close to the full-rank input features (Jing et al., 2022), as shown in Figure 1 (b). The residual connections pave the way for eliminating the dimensional collapse for deep neural networks and indicate the de-oversmoothing probability for deep graph neural networks, but for non-IID graph data, we find the vanilla residual connections can produce sub-optimal results for possible two reasons. First, the vanilla residual connections ignore the topological assumption of graph data that *closer neighbors are more important during the embedding process*, simply adding residual connection can induce “*shading neighbors*” effects, i.e., even residually connected, close neighbors becomes less important during the neural representation process, as we discussed in Section 2.3. Second, targeting this specific oversmoothing phenomenon in the graph representation learning domain, the direct observation is that individual representations are indistinguishable. Hence, contrastive learning serves as a viable solution, but the existing work (Guo et al., 2023) simply introduces vanilla contrastive loss as a regularization while failing to consider the topological relationship of positive and negative pairs.

Facing the latent dimensional collapse problem (i.e., by computing the singular value of covariance matrix of representations) and observable oversmoothing problem (i.e., by discriminating node embedding vectors) in deep graph neural networks, we propose two effective directions, i.e., Weight-Decaying Graph Residual Connection (WG-ResNet) and Structure-Guided Contrastive Loss (SCL). In brief, WG-ResNet adapts weighted residual connections to preserve the input graph topology, and SCL weighs different positive and negative pairs based on their topological relations. The effectiveness of SCL and WG-ResNet in addressing dimensional collapse is also shown in Figure 1 (a). Moreover, it can be observed that SCL itself can alleviate the dimensional collapse to some extent, i.e., addressing oversmoothing by contrastive learning addresses the dimensional collapse, which again proves the unity of dimensional collapse and oversmoothing as we discussed above.

In the end, we propose an end-to-end graph neural network model GearGNN, which encloses SCL and WG-ResNet in a GNN-agnostic manner to help arbitrary graph neural networks go deeper effectively compared with state-of-the-art baselines with theoretical and empirical analysis. Furthermore, we designed extensive ablation studies to show that SCL and WG-ResNet contribute excursively to alleviate the dimensional collapse of the deep graph neural networks for the de-oversmoothing, and their combination can reach optimal results.

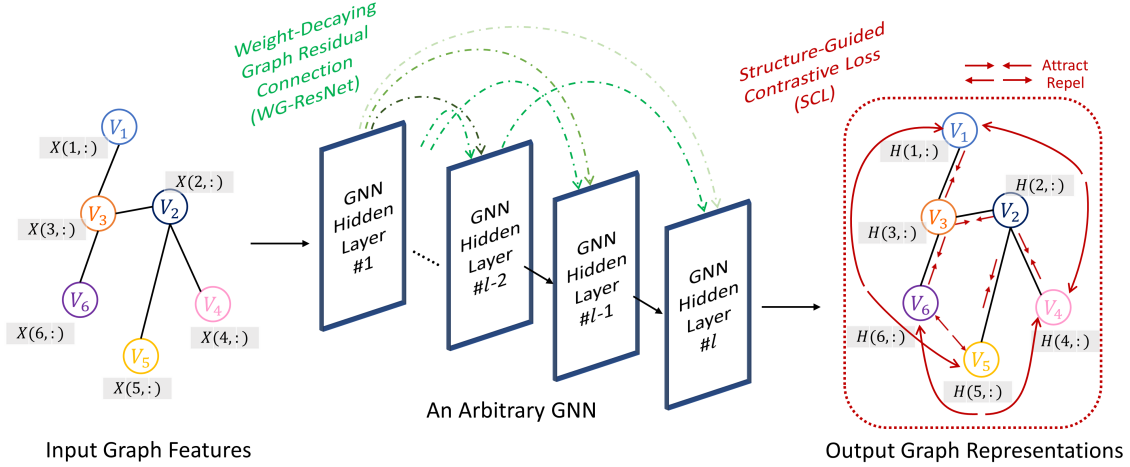


Figure 2: An arbitrary GNN with the proposed GearGNN.

2 Proposed Method

In this section, we begin with the overview of GearGNN and then provide the details of the Weight-decaying Graph Residual Connection (WG-ResNet) and Structure-guided Contrastive Loss (SCL). We formalize the graph embedding problem in the context of an undirected graph $\mathcal{G} = (V, E, \mathbf{X})$, where V consists of n nodes, E consists of m edges, $\mathbf{X} \in \mathbb{R}^{n \times d}$ denotes the feature matrix and d is the feature dimension. We let $\mathbf{A} \in \mathbb{R}^{n \times n}$ denote the adjacency matrix and denote $\mathbf{A}_i \in \mathbb{R}^n$ as the adjacency vector for node v_i . $\mathbf{H}_i \in \mathbb{R}^h$ is the hidden representation vector of v_i .

2.1 Overview of GearGNN

The overview of our proposed GearGNN is shown in Figure 2 and GearGNN consists of two parts, including the graph architecture WG-ResNet and contrastive loss SCL. Specifically, the green dash line stands for WG-ResNet, where $\mathbf{H}^{(l)}$ at the l -th layer will be adjusted by its second last layer $\mathbf{H}^{(l-2)}$ and the first layer $\mathbf{H}^{(1)}$ with proper weights. The red dash line in Figure 2 stands for SCL, where we first sample positive node pairs and negative node pairs based on the input graph topology such that the hidden representations of positive node pairs get closer and negative ones are pushed farther apart. The overall of GearGNN in terms of loss functions and architectures is expressed as follows.

$$\mathcal{L}_{\text{GearGNN}} = \mathcal{L}_{\text{GNN}} + \alpha \mathcal{L}_{\text{SCL}} \quad (1)$$

where \mathcal{L}_{GNN} denotes the loss of the downstream task (e.g., node classification) using an arbitrary GNN model (e.g., GCN (Kipf & Welling, 2017)) equipped with WD-ResNet, \mathcal{L}_{SCL} is the structure-guided contrastive loss, and α is a constant hyperparameter. The details of WG-ResNet and SCL are introduced below.

2.2 Weight-Decaying Graph Residual Connection (WG-ResNet)

As shown in Figure 1 (b), the vanilla residual connections (e.g., ResNet (He et al., 2016)) have the potential to alleviate the dimensional collapse of deep neural networks. But for deep graph neural networks, we discover that simply adding residual connections leads to the sub-optimal solution. As ResNet stacks layers, the importance of close neighbors' features gradually decreases during the GNN information aggregation process, and the faraway neighbor information becomes dominant. More concretely speaking, taking graph convolutional neural network (Kipf & Welling, 2017) as an example, the graph residual connection is expressed as follows.

$$\mathbf{H}^{(l)} = \sigma(\hat{\mathbf{A}}\mathbf{H}^{(l-1)}\mathbf{W}^{(l-1)}) + \mathbf{H}^{(l-2)} \quad (2)$$

where $l(\geq 2)$ denotes the index of layers, $\mathbf{H}^{(l-1)}$ and $\mathbf{H}^{(l-2)}$ are the hidden representations at corresponding layers, $\sigma(\cdot)$ is the activation function, $\mathbf{W}^{(l-1)}$ is the learnable weight matrix, and $\hat{\mathbf{A}}$ is the re-normalized self-looped adjacency matrix with $\hat{\mathbf{A}} = \tilde{\mathbf{D}}^{-\frac{1}{2}} \tilde{\mathbf{A}} \tilde{\mathbf{D}}^{-\frac{1}{2}}$ and $\tilde{\mathbf{A}} = \mathbf{A} + \mathbf{I}$, where $\tilde{\mathbf{D}}$ is the degree matrix. In ResNet, the residual connection connects the current layer and its second last layer. Without loss of generality, we assume the last layer of GNNs is stacked by ResNet, i.e., l is divisible by 2. Then, by extending $\mathbf{H}^{(l-2)}$ iteratively (i.e., substituting it with its previous residual blocks), the above Eq. 2 could be rewritten as follows.

$$\begin{aligned} \mathbf{H}^{(l)} &= \sigma(\hat{\mathbf{A}}\mathbf{H}^{(l-1)}\mathbf{W}^{(l-1)}) + \sigma(\hat{\mathbf{A}}\mathbf{H}^{(l-3)}\mathbf{W}^{(l-3)}) + \mathbf{H}^{(l-4)} \\ &= \underbrace{\sigma(\hat{\mathbf{A}}\mathbf{H}^{(l-1)}\mathbf{W}^{(l-1)}) + \sigma(\hat{\mathbf{A}}\mathbf{H}^{(l-3)}\mathbf{W}^{(l-3)}) + \dots}_{\text{Information aggregated from the faraway neighbors}} + \underbrace{\sigma(\hat{\mathbf{A}}\mathbf{H}^{(i)}\mathbf{W}^{(i)}) + \dots + \sigma(\hat{\mathbf{A}}\mathbf{H}^{(1)}\mathbf{W}^{(1)})}_{\text{Information aggregated from the nearest neighbors}} \end{aligned} \quad (3)$$

According to (Xu et al., 2019), stacking l layers and getting $\mathbf{H}^{(l)}$ in GNNs can be interpreted as aggregating l -hop neighbors' feature information for the node hidden representations. As shown in Eq. 3, when we stack more layers in GNNs, the information collected from faraway neighbors becomes dominant (as there are more terms regarding the information from faraway neighbors), and dilutes the information collected from the nearest neighbors (e.g., 1-hop or 2-hop neighbors). This phenomenon contradicts the general intuition that the close neighbors of a node carry the most important information, and the importance degrades with faraway neighbors. Formally, we describe this phenomenon as *shading neighbors* effect when stacking graph neural layers, as the importance of the nearest neighbors is diminishing. We empirically show that *shading neighbors* effect downgrades the GNNs performance in downstream tasks in Section 3.4. In brief, we show that (1) vanilla ResNet has the shading neighbors effect on graph representation learning; (2) jumping knowledge (Xu et al., 2018) can be a viable solution to the shading neighbors effect; (3) our WG-ResNet achieves the best effectiveness for addressing the shading neighbors effect.

To formally introduce our proposed generic graph architecture, i.e., Weight-Decaying Graph Residual Connection (WG-ResNet). Here, we first introduce the formulation and then provide insights regarding why it can address the problem. Specifically, WG-ResNet introduces the layer similarity and weight decaying factor as follows.

$$\begin{aligned} \tilde{\mathbf{H}}^{(l)} &= \sigma(\hat{\mathbf{A}}\mathbf{H}^{(l-1)}\mathbf{W}^{(l-1)}) \\ \mathbf{H}^{(l)} &= \text{sim}(\mathbf{H}^{(1)}, \tilde{\mathbf{H}}^{(l)}) \cdot e^{-l/\lambda} \cdot \tilde{\mathbf{H}}^{(l)} + \mathbf{H}^{(l-2)} \\ &= e^{\cos(\mathbf{H}^{(1)}, \tilde{\mathbf{H}}^{(l)}) - l/\lambda} \cdot \tilde{\mathbf{H}}^{(l)} + \mathbf{H}^{(l-2)} \end{aligned} \quad (4)$$

where $\cos(\mathbf{H}^{(1)}, \tilde{\mathbf{H}}^{(l)}) = \frac{1}{n} \sum_i \frac{\mathbf{H}_i^{(1)}(\tilde{\mathbf{H}}_i^{(l)})^\top}{\|\mathbf{H}_i^{(1)}\| \|\tilde{\mathbf{H}}_i^{(l)}\|}$ measures the similarity between the l -th layer and the 1-st layer, and we use the exponential function to map the cosine similarity ranging from $[-1, 1]$ to $[e^{-1}, e^1]$, to avoid the negative similarity weights. The term $e^{-l/\lambda}$ is the decaying factor to further adjust the similarity weight of $\tilde{\mathbf{H}}^{(l)}$, where λ is a constant hyperparameter.

Different from the vanilla ResNet (He et al., 2016), we add the learnable similarity $\text{sim}(\mathbf{H}^{(1)}, \tilde{\mathbf{H}}^{(l)})$ to essentially expand the hypothesis space of deeper GNNs. As we mentioned earlier, simply adding vanilla ResNet on GNNs will cause the shading neighbors effect. The introduced decaying factor $e^{-l/\lambda}$ can alleviate this negative effect because it brings the layer-wise dependency to stacking operations and preserves the graph hierarchical information when GNNs go deeper. Since λ is a constant, the value of $e^{-l/\lambda}$ is decreasing as l increases. Thus, the later stacked layer is always less important than previously stacked ones by the decaying weight, which addresses the shading neighbors effect. Without the decaying factor, the layer-wise weights are independent, and the shading neighbors effect can still exist. Moreover, we visualize the layer-wise weight distribution of different residual connection methods (including our WG-ResNet) and their effectiveness in addressing the shading neighbors effect in Appendix B. From another perspective, the hyperparameter λ of the decaying factor actually controls the number of effective neural layers in deeper GNNs. We find its optimal value directly related to the diameter of the input graph, the detailed discussion can be found in Section 3.6.

2.3 Structure-Guided Contrastive Loss (SCL)

According to (Hua et al., 2021; Jing et al., 2022), contrastive representation learning methods show success in preventing dimensional collapse for image recognition whereby representation vectors shrink along certain directions. For graph structure representation learning, the contrastive methods are able to construct the positive and negative sets, and minimizing the similarity of the negative pairs allows the node representations to be uniformly distributed in the embedding space (Wang & Isola, 2020), and some nascent of contrastive learning on graphs have obtained promising alleviation in addressing the dimensional collapse and the corresponding oversmoothing (Zhao & Akoglu, 2020; Guo et al., 2023). However, simply adopting the idea of contrastive regularization in deep graph neural networks could not fully alleviate the dimensional collapse issue due to ignoring the topological relation of non-IID graph data. Thus, how to alleviate dimensional collapse for deep graph neural networks still remains a great challenge. To address this issue with the geometry consideration, we propose the Structure-guided Contrastive Loss (SCL) as follows.

$$\begin{aligned} \mathcal{L}_{\text{SCL}} &= -\mathbb{E}_{v_i \sim V} [\mathbb{E}_{v_j \in \mathcal{N}_i} (\sigma_{ij} \log(f(\mathbf{z}_i, \mathbf{z}_j))) + \mathbb{E}_{v_k \in \bar{\mathcal{N}}_i} (\gamma_{ik} \log(1 - f(\mathbf{z}_i, \mathbf{z}_k)))] \\ \sigma_{ij} &= \frac{n^2}{m} \cdot \frac{1 - \text{dist}(\mathbf{A}_i, \mathbf{A}_j)/n}{\sum_{i,j} (1 - \text{dist}(\mathbf{A}_i, \mathbf{A}_j)/n)}, \quad \gamma_{ik} = \frac{n^2}{n^2 - m} \cdot \frac{1 + \text{dist}(\mathbf{A}_i, \mathbf{A}_k)/n}{\sum_{i,k} (1 + \text{dist}(\mathbf{A}_i, \mathbf{A}_k)/n)} \end{aligned} \quad (5)$$

where $\mathbf{z}_i = g(\mathbf{H}_i^{(l)})$, $g(\cdot)$ is an encoder mapping $\mathbf{H}_i^{(l)}$ to another latent space, $f(\cdot)$ is a similarity function (e.g., $f(a, b) = \exp(\frac{ab^\top}{\|a\| \|b\|})$), $\text{dist}(\cdot)$ is a distance measurement function (e.g., hamming distance (Norouzi et al., 2012)), \mathcal{N}_i is the set containing one-hop neighbors of node v_i , $\bar{\mathcal{N}}_i$ is the complement of the set \mathcal{N}_i , m is the number of edges and n is the number of vertices. In Eq. 5, the directly connected nodes (v_i, v_j) form the positive pair, while not directly connected nodes (v_i, v_k) form the negative pair.

The intuition of Eq. 5 is to maximize the similarity of the representations of the positive pairs and to minimize the similarity of the representations of the negative pairs, such that the node representations become discriminative. In which process, some research works (Perozzi et al., 2014; Grover & Leskovec, 2016; Le, 2021) would first assume that the importance of each edge is identical. However, such an assumption does not always get satisfied in many applications (Velickovic et al., 2017; Faisal et al., 2015). To address this issue, we reweight the importance of edges by considering the graph topological structure via σ and γ . Therefore, for a positive pair, if two nodes have similar topological structures, the weight (i.e., σ) of this node pair should be large; for a negative pair, if two nodes have similar topological structures, the weight (i.e., γ) of this node pair should be small.

Next, we show the importance of these topology-aware weights (i.e., σ and γ) in addressing the oversmoothing issue with the theoretical analysis. For delivering the following analysis clearly, we also consider the node v_i as the anchor node to illustrate, without loss of generality Zhu et al. (2021). Mathematically, some works (Perozzi et al., 2014; Grover & Leskovec, 2016; Le, 2021) assume the importance of each edge is identical, i.e., the edge distribution $P(e)$ is uniform. Thus, we aim to first reweight the importance of edges by considering the graph’s topological information and then deliver the following topology-aware distribution.

To begin with, we denote the probability of sampling a connection e_{ij} and it is a positive connection (i.e., the sampled pair of two nodes v_i and v_j connect in the input graph) as $\tilde{P}_{pos}(e_{ij}) \propto P(e_{ij}, y = 1)$. Then, $\tilde{P}_{pos}(e_{ij})$ can be further extended as $\tilde{P}_{pos}(e_{ij}) = \sigma_{ij} P_{pos}(e_{ij})$, where $P_{pos}(e_{ij}) = \frac{m}{n^2}$ is the prior probability of sampling positive connections, such that σ_{ij} can be interpreted as the conditional probability for the joint probability $\tilde{P}_{pos}(e_{ij})$. Note that a positive connection (e.g., e_{ij}) stands for two connected nodes v_i and v_j forming a positive pair. Similarly, for disconnected two nodes v_i and v_k (i.e., the negative pair or negative connection e_{ik}), we denote $\tilde{P}_{neg}(e_{ik}) = \gamma_{ik} P_{neg}(e_{ik})$, where $P_{neg}(e_{ik}) = 1 - \frac{m}{n^2}$ is the prior probability of sampling a negative connection, and we interpret γ_{ik} as the conditional probability for the joint probability $\tilde{P}_{neg}(e_{ik})$.

Finally, we denote θ to be the parameters of the multi-layer GNN model $\mathcal{G}_\theta(\cdot)$, i.e., $Z = \mathcal{G}_\theta(A, X)$, such that we can prove that SCL could address the oversmoothing issue from the perspective of generative adversarial network (GAN) (Goodfellow et al., 2014) as follows.

Lemma 2.1. \mathcal{L}_{SCL} is a generative adversarial network (GAN) based contrastive learning loss, which could be written as follows.

$$\min_{\theta} \mathcal{L}_{SCL} = \max_{\theta} \int_e (\tilde{P}_{pos}(e) \log(D(e)) + \tilde{P}_{neg}(e) \log(1 - D(e))) de$$

where $D(e) = f(\mathbf{z}_i, \mathbf{z}_j)$ is the discriminator of GAN with edge $e = (v_i, v_j)$, node representations \mathbf{z}_i and \mathbf{z}_j . $\tilde{P}_{pos}(e) = \sigma P_{pos}(e)$ and $\tilde{P}_{neg}(e) = \gamma P_{neg}(e)$. (Proof in Appendix C)

Theorem 2.2. \mathcal{L}_{SCL} can address the oversmoothing problem, given the optimal discriminator in Lemma 2.1.

Proof. Based on Lemma 2.1 and following Theorem 1 in GAN (Goodfellow et al., 2014), the optimal $D^*(e)$ is given by $D^*(e) = \frac{\tilde{P}_{pos}(e)}{\tilde{P}_{pos}(e) + \tilde{P}_{neg}(e)}$. Since $\tilde{P}_{pos}(e_{ij}) = \sigma_{ij} P_{pos}(e_{ij})$ and $\tilde{P}_{neg}(e_{ik}) = \gamma_{ik} P_{neg}(e_{ik})$, we have

$$\begin{aligned} D^*(e) &= \frac{\sigma * P_{pos}(e)}{\sigma * P_{pos}(e) + \gamma * P_{neg}(e)} \\ &= \frac{P(e|y=1)P(y=1)}{P(e|y=1)P(y=1) + P(e|y=0)P(y=0)} \\ &= P(y=1|e) \end{aligned}$$

Therefore, $D(e)$ can be interpreted as maximizing the conditional log-likelihood $P(y=1|e)$, where y indicates whether edge e (or a node pair) is positive or negative.

Notice that the discriminator $D(e)$ is defined as the similarity measurement of a node pair in Lemma 2.1. If $D(e)$ is able to distinguish whether a node pair is a negative pair or not, the hidden representations of these two nodes (negative pair) are distinguishable. Therefore, we can conclude that when \mathcal{L}_{SCL} achieves the optimal solution, the model could successfully discriminate the difference of the embeddings for the negative pairs, thus addressing the oversmoothing issue. In practice, the optimum is usually approximated by the model convergence. \square

3 Experiments

In this section, we comprehensively demonstrate the performance of our proposed GearGNN compared with state-of-the-art deeper graph neural networks and self-ablations, trying to answer the following research questions.

- RQ1: When do we need more layers of graph neural networks? (*Answered in Section 3.2*)
- RQ2: When it is necessary to be deep, can the proposed GearGNN address dimensional collapse and oversmoothing to outperform? (*Answered in Section 3.3*)
- RQ3: Is every component of GearGNN helpful and irreplaceable? (*Answered in Section 3.4*)
- RQ4: In practice, can GearGNN be agnostic to help various off-the-shelf graph neural network architectures? (*Answered in Section 3.5*)

3.1 Experiment Setup

Datasets. *Cora* (Lu & Getoor, 2003) dataset is a citation network consisting of 5,429 edges and 2,708 scientific publications from 7 classes. The edge in the graph represents the citation of one paper by another. *CiteSeer* (Lu & Getoor, 2003) dataset consists of 3,327 scientific publications which could be categorized into 6 classes, and this citation network has 9,228 edges. *PubMed* (Namata et al., 2012) is a citation network consisting of 88,651 edges and 19,717 scientific publications from 3 classes. *Reddit* (Hamilton et al., 2017b) dataset is extracted from Reddit posts, which consists of 4,584 nodes and 19,460 edges. Notice that we follow the splitting strategy used in (Zhao & Akoglu, 2020) by randomly sampling 3% of the nodes as the training samples, 10% of the nodes as the validation samples, and the remaining 87% as the test samples.

OGB-arXiv (Wang et al., 2020) is a citation network, which consists of 1,166,243 edges and 169,343 nodes from 40 classes.

Baselines. We compare the performance of our method with the following baselines including one vanilla GNN model and four state-of-the-art deeper GNN models: (1) GCN (Kipf & Welling, 2017): the vanilla graph convolutional network; (2) GCNII (Chen et al., 2020): an extension of GCN with skip connections and additional identity matrices; (3) DGN (Zhou et al., 2020): the differentiable group normalization for GNNs to normalize nodes within the same group and separate nodes among different groups; (4) PairNorm (Zhao & Akoglu, 2020): a GNN normalization layer designed to prevent node representations from becoming too similar; (5) DropEdge (Rong et al., 2020): a GNN-agnostic framework that randomly removes a certain number of edges from the input graph; (6) RevGCN-Deep (Li et al., 2021): equilibrium model based deep graph neural networks; (7) EGNN (Zhou et al., 2021): dirichlet energy constrained deep graph neural networks; (8) ContraNorm (Guo et al., 2023): a contrastive learning-based layer normalization method.

Configurations. For a fair comparison, we set the dropout rate to 0.5, the weight decay rate to 0.0005, and the total number of iterations to 1500 for all methods; if not specialized, GCN is chosen as the backbone, and the dimension of each layer is set to 50 for all the graph neural network baseline methods. In Section 3.4, for GearGNN and GearGNN-S, we sample 10 instances and 5 neighbors for each class from the training set, $dist(\cdot)$ is the hamming distance, and $f(\cdot)$ is the cosine similarity measurement. The experiments are repeated 10 times if not otherwise specified. All of the real-world datasets are publicly available. The experiments are performed on a Windows machine with a 16GB RTX 5000 GPU. Detailed reproducibility with released code can be found in Appendix D.

3.2 When do we need more layers of graph neural networks?

Case 1: Missing Features. We first imagine a scenario where some values of attributes are missing in the input graph. In this scenario, the shallow GNNs may not work well because GNNs could not collect useful information from the neighbors due to the massive missing values. However, if we increase the number of layers, GNNs are able to gather more information from the k -hop neighbors and capture latent knowledge to compensate for missing features. To verify this, we conduct the following experiment: we randomly mask $p\%$ attributes on Cora and CiteSeer datasets (i.e., setting the masked attributes to be 0), gradually increase the number of layers, and record the accuracy for each setting following (Zhao & Akoglu, 2020). In this case study, the number of layers is selected from $\{2, 3, 4, 5, 6, 7, 8, 9, 10, 15, 20, 25, 30, 40, 50, 60\}$, and the backbone model is GCN. For a fair comparison, we add ResNet (He et al., 2016) if it can boost the baseline model’s performance. We repeat the experiments five times and record the mean accuracy and standard deviation.

Table 1: Node Classification on Two Datasets by Masking $p\%$ of Input Node Attributes (L denotes the number of layers where a model achieves the best performance).

| Node Feature Missing Rate | | $p = 25\%$ | | $p = 50\%$ | | $p = 75\%$ | |
|---------------------------|---------------------|---------------------------------------|-----|---------------------------------------|-----|---------------------------------------|-----|
| dataset | Method | Accuracy | L | Accuracy | L | Accuracy | L |
| Cora | GCN + ResNet | 0.7503 ± 0.0101 | 7 | 0.7435 ± 0.0048 | 10 | 0.7226 ± 0.0099 | 10 |
| | PairNorm + ResNet | 0.7529 ± 0.0129 | 10 | 0.7482 ± 0.0172 | 20 | 0.7262 ± 0.0178 | 40 |
| | DropEdge + ResNet | 0.7634 ± 0.0112 | 15 | 0.7611 ± 0.0102 | 20 | 0.7297 ± 0.0168 | 8 |
| | GCNII + ResNet | 0.2667 ± 0.0063 | 25 | 0.3351 ± 0.0066 | 25 | 0.2914 ± 0.0106 | 40 |
| | DGN w/o ResNet | 0.6850 ± 0.0184 | 30 | 0.6846 ± 0.0147 | 50 | 0.6717 ± 0.0156 | 25 |
| | ContraNorm + ResNet | 0.7319 ± 0.0099 | 2 | 0.7189 ± 0.0091 | 3 | 0.6902 ± 0.0107 | 3 |
| | GearGNN | 0.7915 ± 0.0060 | 10 | 0.7848 ± 0.0043 | 20 | 0.7598 ± 0.0081 | 60 |
| CiteSeer | GCN + ResNet | 0.6141 ± 0.0080 | 4 | 0.5811 ± 0.0093 | 10 | 0.5149 ± 0.0173 | 9 |
| | PairNorm + ResNet | 0.6184 ± 0.0087 | 8 | 0.5947 ± 0.0083 | 20 | 0.5176 ± 0.0075 | 10 |
| | DropEdge + ResNet | 0.6348 ± 0.0156 | 4 | 0.6083 ± 0.0128 | 6 | 0.5240 ± 0.0128 | 10 |
| | GCNII + ResNet | 0.2453 ± 0.0045 | 40 | 0.2338 ± 0.0028 | 20 | 0.2403 ± 0.0046 | 25 |
| | DGN w/o ResNet | 0.4560 ± 0.0162 | 20 | 0.4593 ± 0.0117 | 15 | 0.4498 ± 0.0292 | 15 |
| | ContraNorm + ResNet | 0.5893 ± 0.0114 | 2 | 0.5621 ± 0.0111 | 3 | 0.4646 ± 0.0076 | 4 |
| | GearGNN | 0.6524 ± 0.0087 | 20 | 0.6169 ± 0.0063 | 60 | 0.5576 ± 0.0070 | 50 |

Table 1 shows the performance of GearGNN and various baselines with the optimal number of layers denoted as $\#L$, i.e., when the model achieves the best performance. By observation, we find that when the missing rate is 25%, shallow GCN with ResNet has enough capacity to achieve the best performance on both CiteSeer and Cora datasets. Compared with GCN, our proposed method further improves the performance by more than 3.83% on the CiteSeer dataset and 4.08% on the Cora dataset by stacking more layers. However, when we increase the missing rate to 50% and 75%, we observe that most methods tend to achieve the best performance by stacking more layers. Specifically, PairNorm achieves the best performance at 10 layers when 25% features are missing, while it has the best performance at 40 layers when 75% features are missing. A similar observation could also be found with GCNII on the Cora dataset, DropEdge on the CiteSeer dataset as well as our proposed methods in both datasets. Overall, the experimental results verify that the more features a dataset are missing, the more layers GNNs need to be stacked to achieve better performance. Our explanation for this observation is that if the number of layers increases, more information will be collected from the k -hop neighbors to recover the missing information of its 1-hop and 2-hop neighbors.

Case 2: Disalignment of topological and feature distribution. Then, we conduct another case study with a toy example that near neighbors may not share similar contents in terms of input features. We first use the existing package (i.e., the `draw_circle` function in the Scikit-learn package) to generate a synthetic dataset by setting the number of data points to 1,000 and the noise level to 0.01. Then, we measure the euclidean distance between each pair of data points, and if the distance is less than a threshold, then these two data points are connected in a graph. In this way, the adjacency matrix is derived after adding the self-loop. Next, we sample 1% data points as the training set, 9% data points as the validation set, and 90% data points as the test set. These data points are visualized in Figure 3a and the experimental results are shown in Figure 3b. In Figure 3a, we observe that the query node (the blue diamond in the dashed circle) cannot rely on its closest labeled neighbor (the red star in the dashed circle) to correctly predict its label (red or blue). Only by exploring longer paths consisting of more similar neighbors are we able to predict its label as blue (i.e., the blue star in the dashed circle). Figure 3b compares the classification accuracy of shallow GNNs and deeper GNNs. We can see that deeper GNNs significantly outperform shallow ones by more than 11%, due to their ability to explore longer paths on the graph.

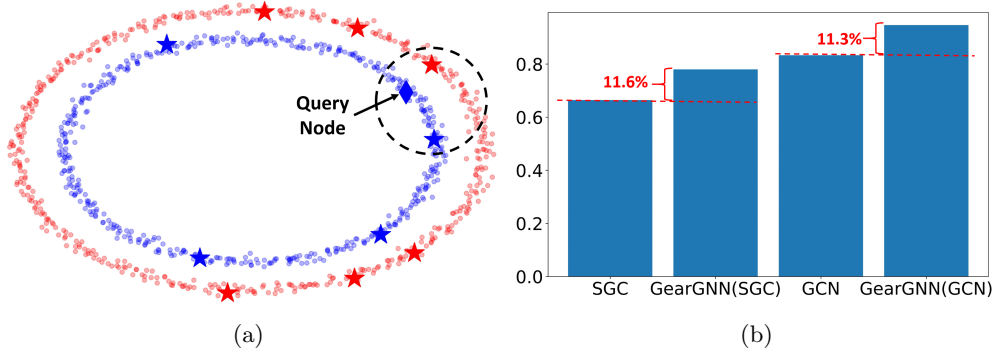


Figure 3: A Toy Example to Demonstrate the Benefit of Deeper GNN Models. (a) Two groups of nodes in the semi-supervised setting. Stars are labeled, dots are unlabeled, and the diamond is the query node. Euclidean distance between two nodes indicates the edge connection. (b) Comparison of node classification accuracy between shallow and deeper GNN models using data on the left. The deeper GNNs are realized by GearGNN with corresponding backbones.

3.3 Effectiveness Analysis of GearGNN

Here, we evaluate the effectiveness of the proposed method on benchmark datasets by comparing it with state-of-the-art methods shown in Table 2. The backbone model for all methods we used in these experiments is GCN (Kipf & Welling, 2017), and for a fair comparison, we set the dimension of the hidden layer to 50 and vary the number of hidden layers from 2 to 16, 32, and 64 for all methods on the small dataset. We also examine the node classification performance of GearGNN on a large-scale dataset OGB-arXiv in Table 3. In

OGB-arXiv, we fix the feature dimension of the hidden layer as 100, the total iteration is set as 3000, and GCN is also chosen as the backbone model. Due to the memory limitation, we only record the performance of all methods by setting the number of layers to 2, 10, and 20, respectively. The experiments are repeated 5 times and we record the mean accuracy as well as the standard deviation.

Table 2: Node Classification on Small Datasets with Varying Layers L (GCN as the Backbone).

| Dataset | Method | $L = 2$ | $L = 16$ | $L = 32$ | $L = 64$ |
|----------|------------|---------------------------------------|---------------------------------------|---------------------------------------|---------------------------------------|
| Cora | GCN | 0.7643 \pm 0.0040 | 0.5262 \pm 0.0732 | 0.3284 \pm 0.0066 | 0.3274 \pm 0.0189 |
| | PairNorm | 0.7818 \pm 0.0027 | 0.6080 \pm 0.0310 | 0.5138 \pm 0.0299 | 0.2932 \pm 0.0120 |
| | DropEdge | 0.7828 \pm 0.0075 | 0.7557 \pm 0.0072 | 0.7306 \pm 0.0134 | 0.2685 \pm 0.0647 |
| | GCNII | 0.6778 \pm 0.0065 | 0.7237 \pm 0.0055 | 0.7142 \pm 0.0015 | 0.7107 \pm 0.0047 |
| | DGN | 0.7545 \pm 0.0003 | 0.6785 \pm 0.0169 | 0.7067 \pm 0.0190 | 0.7104 \pm 0.0192 |
| | ContraNorm | 0.7682 \pm 0.0044 | 0.6590 \pm 0.0291 | 0.5128 \pm 0.0241 | 0.4328 \pm 0.0320 |
| | GearGNN | 0.7768 \pm 0.0057 | 0.8002 \pm 0.0058 | 0.7961 \pm 0.0055 | 0.8022 \pm 0.0061 |
| CiteSeer | GCN | 0.6452 \pm 0.0072 | 0.4514 \pm 0.0987 | 0.2689 \pm 0.0099 | 0.2680 \pm 0.0093 |
| | PairNorm | 0.6030 \pm 0.0153 | 0.2268 \pm 0.0398 | 0.2096 \pm 0.0029 | 0.2076 \pm 0.0033 |
| | DropEdge | 0.6532 \pm 0.0068 | 0.6117 \pm 0.0229 | 0.5101 \pm 0.0430 | 0.2138 \pm 0.0198 |
| | GCNII | 0.5912 \pm 0.0106 | 0.6180 \pm 0.0031 | 0.6159 \pm 0.0019 | 0.6101 \pm 0.0017 |
| | DGN | 0.4872 \pm 0.0168 | 0.4753 \pm 0.0591 | 0.4604 \pm 0.0162 | 0.4417 \pm 0.0219 |
| | ContraNorm | 0.6263 \pm 0.0061 | 0.4621 \pm 0.0237 | 0.3965 \pm 0.0196 | 0.2128 \pm 0.0208 |
| | GearGNN | 0.6577 \pm 0.0065 | 0.6650 \pm 0.0059 | 0.6655 \pm 0.0031 | 0.6685 \pm 0.0066 |
| PubMed | GCN | 0.7990 \pm 0.0017 | 0.5383 \pm 0.0200 | 0.5463 \pm 0.0391 | 0.5566 \pm 0.0086 |
| | PairNorm | 0.8120 \pm 0.0076 | 0.4408 \pm 0.0683 | 0.3972 \pm 0.0094 | 0.3960 \pm 0.0097 |
| | DropEdge | 0.8035 \pm 0.0020 | 0.7893 \pm 0.0042 | 0.7902 \pm 0.0032 | 0.3951 \pm 0.0108 |
| | GCNII | 0.8070 \pm 0.0009 | 0.8094 \pm 0.0010 | 0.8089 \pm 0.0007 | 0.8097 \pm 0.0009 |
| | DGN | 0.7947 \pm 0.0358 | 0.7553 \pm 0.0295 | 0.7733 \pm 0.0143 | 0.7632 \pm 0.0226 |
| | ContraNorm | 0.8061 \pm 0.0020 | 0.5672 \pm 0.0684 | 0.4348 \pm 0.0379 | 0.3971 \pm 0.0057 |
| | GearGNN | 0.8175 \pm 0.0016 | 0.8097 \pm 0.0038 | 0.8098 \pm 0.0025 | 0.8109 \pm 0.0033 |
| Reddit | GCN | 0.8757 \pm 0.0054 | 0.8540 \pm 0.0451 | 0.3655 \pm 0.0251 | 0.3410 \pm 0.0288 |
| | PairNorm | 0.7704 \pm 0.0052 | 0.8636 \pm 0.0448 | 0.6468 \pm 0.0429 | 0.1230 \pm 0.0299 |
| | DropEdge | 0.8564 \pm 0.0059 | 0.8526 \pm 0.0046 | 0.5384 \pm 0.1049 | 0.1053 \pm 0.0148 |
| | GCNII | 0.6184 \pm 0.0108 | 0.7157 \pm 0.0016 | 0.6972 \pm 0.0039 | 0.6963 \pm 0.0059 |
| | DGN | 0.7829 \pm 0.0137 | 0.7397 \pm 0.0371 | 0.6806 \pm 0.0639 | 0.5058 \pm 0.0754 |
| | ContraNorm | 0.6576 \pm 0.0094 | 0.2563 \pm 0.0091 | 0.2547 \pm 0.0170 | 0.2664 \pm 0.0140 |
| | GearGNN | 0.8762 \pm 0.0060 | 0.9676 \pm 0.0033 | 0.9693 \pm 0.0023 | 0.9721 \pm 0.0011 |

Table 3: Node Classification on Large Dataset with Varying Layers L (GCN as the Backbone).

| Dataset | Method | $L = 2$ | $L = 10$ | $L = 20$ |
|-----------|------------|---------------------------------------|---------------------------------------|---------------------------------------|
| OGB-arXiv | GCN | 0.7136 \pm 0.0044 | 0.7021 \pm 0.0018 | 0.5377 \pm 0.0756 |
| | PairNorm | 0.7186 \pm 0.0008 | 0.7158 \pm 0.0035 | 0.5796 \pm 0.0090 |
| | DropEdge | 0.7178 \pm 0.0012 | 0.6531 \pm 0.0056 | 0.2198 \pm 0.0097 |
| | GCNII | 0.5966 \pm 0.0013 | 0.6340 \pm 0.0017 | 0.6246 \pm 0.0015 |
| | DGN | 0.6039 \pm 0.0037 | 0.5746 \pm 0.0033 | 0.5027 \pm 0.0056 |
| | ContraNorm | 0.7294 \pm 0.0025 | 0.6941 \pm 0.0030 | 0.5821 \pm 0.0324 |
| | GearGNN | 0.7369 \pm 0.0014 | 0.7386 \pm 0.0006 | 0.7401 \pm 0.0009 |

Based on the observation in Table 2 and Table 3, we find that (1) many existing graph de-over-smoothing methods (e.g., PairNorm, ContraNorm) achieve the best performance with the shallow layer (i.e., $L = 2$), and the performance of these methods begin to decrease as we increase the number of layers; (2) GearGNN outperforms all baseline methods when we stack the layers of GNN (i.e., $L = 16$, $L = 32$ and $L = 64$); (3) when we set 64-layer GCN as the reference, DropEdge, DropEdge, and ContraNorm have worse performance than the vanilla GCN; (4) GCNII, DGN, and GearGNN boost the performance by more than 150% on average compared with GCN; (5) GCNII and GearGNN perform better with deep graph architecture (e.g., $L = 32$ or $L = 64$); (6) the performance of GearGNN on OGB-arXiv dataset increases as we stack layers, which verifies our conjecture that increasing the number of layers indeed leads to better performance in large graphs due to more information aggregated from neighbors; (7) when we set the number of layers to

10 for the OGB-arXiv dataset, the performance of most of these baseline methods start to drop and the performance of these methods deteriorate rapidly as we further stack layers. Additional comparison with RevGCN-Deep and EGNN can be found in Appendix E.

In addition to Table 2 and Table 3, we also visualize the corresponding number of the nonzero singular values on those datasets in Figure 4. In Figure 4, taking Cora and OGB-arXiv as examples, we observe that (1) PairNorm and ContraNorm begin to suffer from the dimensional collapse issue on both datasets when the number of layers is greater than 10; (2) Dropedge, DGN, and GCNII perform well on the small dataset but fail to preserve the full-rank representation on the large dataset; (3) the node representations by GearGNN are full-rank on both datasets, which indicates that GearGNN could alleviate dimensional collapse.

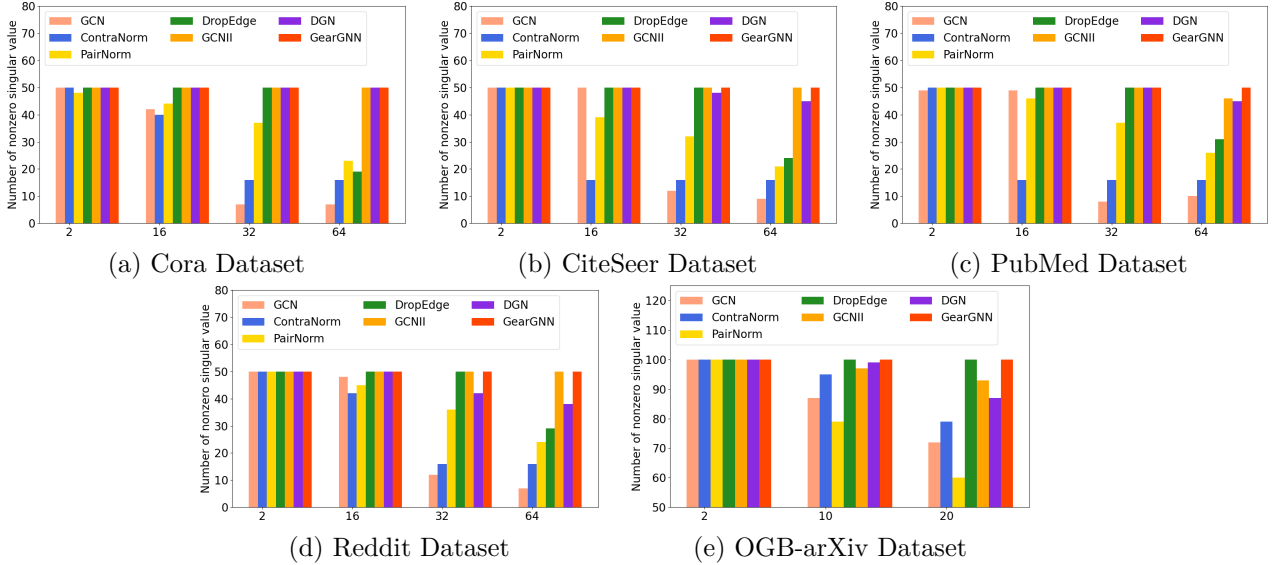


Figure 4: The x -axis is the number of layers and the y -axis is the number of the non-zero singular values of the covariance matrix of the node representations by different methods.

Combined with the observation in Figure 4, Table 2 and Table 3, most of the baseline methods suffer from the dimensional collapse issue and not fully address the oversmoothing problem when we stack graph neural network layers, while our proposed GearGNN could largely alleviate the dimensional collapse issue in terms of both node classification performance and the singularity ranking.

3.4 Ablation Study of GearGNN

Here, we conduct the ablation study to show the effectiveness and irreplaceability of WG-ResNet and SCL in Table 4. In this experiment, we fix the total iteration set as 3000, and GCN is chosen as the backbone model. For the Cora dataset, the feature dimension of the hidden layer is 50 and the number of layers is 64; for the OGB-arXiv dataset the feature dimension of the hidden layer is 100 and the number of layers is 20. In Table 4, GearGNN-T removes SCL, GearGNN-D removes the weight decaying factor in WG-ResNet and GearGNN-JK replaces the WG-ResNet by Jumping Knowledge (Xu et al., 2018).

Table 4: Ablation Study w.r.t. Node Classification Accuracy.

| Method | Cora ($L = 64$) | CiteSeer ($L = 64$) | PubMed ($L = 64$) | Reddit ($L = 64$) | OGB-arXiv ($L = 20$) |
|------------|---------------------------------------|---------------------------------------|---------------------------------------|---------------------------------------|---------------------------------------|
| GCN+RseNet | 0.7252 ± 0.0176 | 0.6213 ± 0.0056 | 0.7985 ± 0.0068 | 0.9432 ± 0.0037 | 0.7144 ± 0.0013 |
| GearGNN-D | 0.7498 ± 0.0139 | 0.6567 ± 0.0052 | 0.8050 ± 0.0031 | 0.9654 ± 0.0028 | 0.7363 ± 0.0011 |
| GearGNN-T | 0.7875 ± 0.0092 | 0.5750 ± 0.0244 | 0.8078 ± 0.0047 | 0.9397 ± 0.0042 | 0.7335 ± 0.0024 |
| GearGNN-JK | 0.7955 ± 0.0078 | 0.6600 ± 0.0085 | 0.8061 ± 0.0038 | 0.9659 ± 0.0046 | 0.7368 ± 0.0012 |
| GearGNN | 0.8022 ± 0.0061 | 0.6685 ± 0.0066 | 0.8109 ± 0.0033 | 0.9721 ± 0.0011 | 0.7401 ± 0.0009 |

In Table 4, we have the following observations (1) comparing GearGNN with GearGNN-T, we find that GearGNN boosts the performance by 1.84% on the Cora dataset after adding SCL, which demonstrates the effectiveness of SCL to address the oversmoothing issue; (2) GearGNN outperforms GearGNN-D on Cora dataset by 5.61%, which shows that GearGNN could address the shading neighbors effect by adding the weight decaying factor; (3) comparing GearGNN with GearGNN-JK, we verify that our proposed WG-ResNet is more effective than GearGNN-JK. Besides, one drawback of jumping knowledge is its high memory required as the number of layers increases, while our proposed WG-ResNet doesn't; (4) GearGNN outperforms GCN+ResNet by more than 7.7% on the Cora dataset and 2.6% on the OGB-arXiv dataset, which indicates that WG-ResNet could alleviate the shading neighbors effect.

3.5 Different Backbones of GearGNN

Here, we show the performance of our proposed GearGNN cooperating with different backbone models (e.g., GAT (Velickovic et al., 2018) and GraphSage (Hamilton et al., 2017a)). In Figure 5, we set the numbers of the hidden layers as 60 for all methods and the dimension of the hidden layer as 50. The total number of training iterations is 1500.

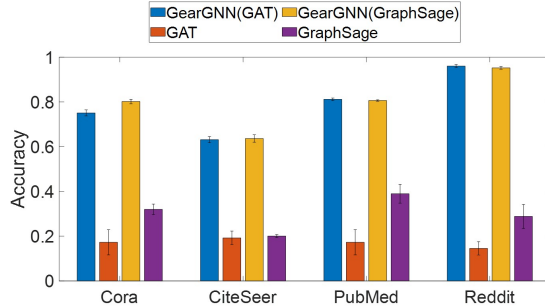


Figure 5: Accuracy of Different Backbone Models with 64 Hidden Layers on Four Datasets.

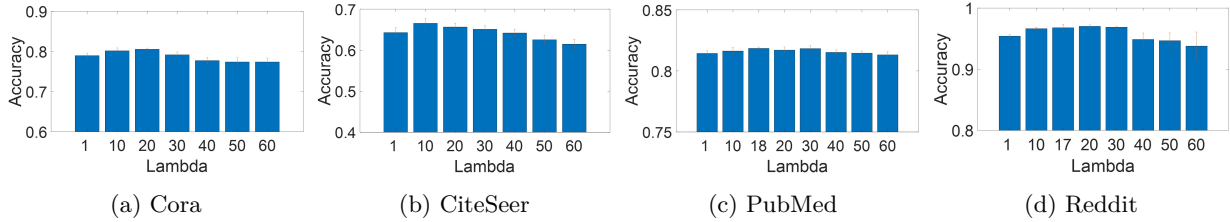
By observation, we find that both GAT and GraphSage suffer from oversmoothing when the architecture becomes deeper, and our proposed method GearGNN greatly alleviates it and boosts the performance by 40%-60% on average over four datasets. Specifically, compared with the vanilla GraphSage, our GearGNN boosts its performance by 43% on the CiteSeer dataset and more than 67% on the Reddit dataset.

3.6 Number of Effective Layers in Deep Graph Neural Networks

We conduct the hyperparameter analysis of GearGNN, regarding λ in the weight decaying function of Eq. 4. For example, when $\lambda = 10$, the decaying factor for the 10-th layer is 0.3679 (i.e., e^{-1}); but for the 30-th layer, it is 0.0049 (i.e., e^{-3}). This decay limits the effective information aggregation scope of deeper GNNs because the later stacked layers will become significantly less important. Based on this controlling property of λ , a natural follow-up question is whether its value depends on the property of input graphs.

Interestingly, through our experiments, we find that *the optimal λ is very close to the diameter of input graphs (if it is connected) or the largest component (if it does not have many separate components)*. This observation verifies our conjecture regarding the property of λ (i.e., it controls the number of effective layers or the number of hops during the message passing aggregation schema of GNNs). Hence, the value of λ can be searched around the diameter of the input graph.

To analyze the hyperparameter λ , we fix the feature dimension of the hidden layer to be 50, the total iteration is set to be 3000, the number of layers is set to be 60, the sampling batch size for GearGNN is 10, and GCN is chosen as the backbone model. The experiment is repeated five times for each configuration. In each sub-figure of Figure 6, the x -axis is the value of λ , and the y -axis is the accuracy of 60-layer GCN in the above setting.

Figure 6: Hyperparameter Analysis, i.e., λ vs Node Classification Accuracy on Four Datasets.

First, we can observe that it’s not true that GearGNN achieves the best performance with a larger λ . Specifically, we find that the optimal $\lambda = 20$ on the Cora dataset, the optimal $\lambda = 10$ on the CiteSeer dataset, the optimal $\lambda = 18$ on the PubMed dataset, and the optimal $\lambda = 20$ on the Reddit dataset. Then, natural questions to ask are (1) *what determines the optimal value of λ in different datasets?* (2) *can we gather some heuristics to narrow down the hyperparameter search space to efficiently establish effective GNNs?*

Thus, we provide our discovery. In Eq. 4, we have analyzed that the decaying factor λ controls the number of effective layers in deeper GNNs by introducing the layer-wise dependency. It means that larger λ slows down the weight decay and gives considerably large weights to more layers such that they can be effective, and the information aggregation scope of GNN extends as more multi-hop neighbor features are collected and aggregated. In graph theory, diameter represents the scope of the graph, which is the largest value of the shortest path between any node pairs in the graph. Therefore, the optimal λ should be restricted by the input graph, i.e., being close to the input graph diameter.

Table 5: Graph Statistics of Each Dataset.

| Metric | Cora | Citeseer | PubMed | Reddit |
|--|-------|----------|--------|--------|
| Number of Nodes | 2,708 | 3,327 | 19,717 | 4,854 |
| Connected Graph | No | No | Yes | Yes |
| Number of Components | 78 | 438 | 1 | 1 |
| Diameter of the Graph (or the Largest Component) | 19 | 28 | 18 | 17 |

Interestingly, our experiments reflect this observation. Combining the optimal λ in Figure 6 and the diameter in Table 5, for connected graphs PubMed and Reddit, the optimal λ is very close to the graph diameter. This also happens to Cora (even though Cora is not connected), because the number of components is not large. As for CiteSeer, the optimal λ is less than the diameter of its largest component. A possible reason is that CiteSeer has many (i.e., 438) small components, which shrinks the information propagation scope, such that we do not need to stack many layers and we do not need to enlarge λ to the largest diameter (i.e., 28). In general, based on the above analysis, we find the optimal value of λ can be searched around the diameter of the input graph.

4 Conclusion

In this paper, we focus on building deeper graph neural networks to effectively model graph data and illustrate the oversmoothing cause from the perspective of dimensional collapse. To address this, we first provide insights regarding why ResNet is not best suited for many deeper graph neural network solutions, i.e., the *shading neighbors* effect. Then we propose a new residual architecture, Weight-decaying Graph Residual Connection (WG-ResNet) to address this effect. In addition, we propose a Structure-guided Contrastive Loss (SCL) to address the problem from another viewpoint, where we utilize graph topological information, pull the representations of connected node pairs closer, and push remote node pairs farther apart via contrastive learning regularization. Combining WG-ResNet with SCL, an end-to-end model GearGNN is proposed for deep graph neural networks. We provide the theoretical analysis of our proposed method and demonstrate the effectiveness of GearGNN by extensive experiment comparing with state-of-the-art methods.

References

- Ming Chen, Zhewei Wei, Zengfeng Huang, Bolin Ding, and Yaliang Li. Simple and deep graph convolutional networks. In *ICML*, 2020.
- John C. Duchi, Elad Hazan, and Yoram Singer. Adaptive subgradient methods for online learning and stochastic optimization. *JMLR*, 2011.
- S. M. Faisal, Georgios Tziantzioulis, Ali Murat Gok, Nikolaos Hardavellas, Seda Ogrenci Memik, and Srinivasan Parthasarathy. Edge importance identification for energy efficient graph processing. In *2015 IEEE International Conference on Big Data (IEEE BigData 2015), Santa Clara, CA, USA, October 29 - November 1, 2015*, pp. 347–354. IEEE Computer Society, 2015.
- Ian J. Goodfellow, Jean Pouget-Abadie, Mehdi Mirza, Bing Xu, David Warde-Farley, Sherjil Ozair, Aaron C. Courville, and Yoshua Bengio. Generative adversarial networks. *CoRR*, abs/1406.2661, 2014. URL <http://arxiv.org/abs/1406.2661>.
- Aditya Grover and Jure Leskovec. node2vec: Scalable feature learning for networks. In Balaji Krishnapuram, Mohak Shah, Alexander J. Smola, Charu C. Aggarwal, Dou Shen, and Rajeev Rastogi (eds.), *Proceedings of the 22nd ACM SIGKDD International Conference on Knowledge Discovery and Data Mining, San Francisco, CA, USA, August 13-17, 2016*, pp. 855–864. ACM, 2016.
- Xiaoju Guo, Yifei Wang, Tianqi Du, and Yisen Wang. Contranorm: A contrastive learning perspective on oversmoothing and beyond. In *The Eleventh International Conference on Learning Representations, ICLR 2023, Kigali, Rwanda, May 1-5, 2023*. OpenReview.net, 2023. URL <https://openreview.net/pdf?id=SM7XkJouWHm>.
- Will Hamilton, Zhitao Ying, and Jure Leskovec. Inductive representation learning on large graphs. *Advances in neural information processing systems*, 30, 2017a.
- William L. Hamilton, Justine Zhang, Cristian Danescu-Niculescu-Mizil, Dan Jurafsky, and Jure Leskovec. Loyalty in online communities. In *Proceedings of the Eleventh International Conference on Web and Social Media, ICWSM 2017, Montréal, Québec, Canada, May 15-18, 2017*, pp. 540–543. AAAI Press, 2017b.
- Kaiming He, Xiangyu Zhang, Shaoqing Ren, and Jian Sun. Deep residual learning for image recognition. In *CVPR*, 2016.
- Tianyu Hua, Wenxiao Wang, Zihui Xue, Sucheng Ren, Yue Wang, and Hang Zhao. On feature decorrelation in self-supervised learning. In *2021 IEEE/CVF International Conference on Computer Vision, ICCV 2021, Montreal, QC, Canada, October 10-17, 2021*, pp. 9578–9588. IEEE, 2021.
- Kexin Huang and Marinka Zitnik. Graph meta learning via local subgraphs. In *NeurIPS*, 2020.
- Li Jing, Pascal Vincent, Yann LeCun, and Yuandong Tian. Understanding dimensional collapse in contrastive self-supervised learning. In *The Tenth International Conference on Learning Representations, ICLR 2022, Virtual Event, April 25-29, 2022*. OpenReview.net, 2022.
- Thomas N. Kipf and Max Welling. Semi-supervised classification with graph convolutional networks. In *ICLR*, 2017.
- Can M. Le. Edge sampling using local network information. *J. Mach. Learn. Res.*, 22:88:1–88:29, 2021.
- Guohao Li, Matthias Müller, Bernard Ghanem, and Vladlen Koltun. Training graph neural networks with 1000 layers. In Marina Meila and Tong Zhang (eds.), *Proceedings of the 38th International Conference on Machine Learning, ICML 2021, 18-24 July 2021, Virtual Event*, volume 139 of *Proceedings of Machine Learning Research*, pp. 6437–6449. PMLR, 2021.
- Qimai Li, Zhichao Han, and Xiao-Ming Wu. Deeper insights into graph convolutional networks for semi-supervised learning. In *AAAI*, 2018.

- Qing Lu and Lise Getoor. Link-based classification. In Tom Fawcett and Nina Mishra (eds.), *Machine Learning, Proceedings of the Twentieth International Conference (ICML 2003), August 21-24, 2003, Washington, DC, USA*, pp. 496–503. AAAI Press, 2003.
- Galileo Namata, Ben London, Lise Getoor, Bert Huang, and U Edu. Query-driven active surveying for collective classification. In *10th International Workshop on Mining and Learning with Graphs*, volume 8, 2012.
- Mohammad Norouzi, David J Fleet, and Russ R Salakhutdinov. Hamming distance metric learning. *Advances in neural information processing systems*, 25, 2012.
- Kenta Oono and Taiji Suzuki. Graph neural networks exponentially lose expressive power for node classification. In *ICLR*, 2020.
- Bryan Perozzi, Rami Al-Rfou, and Steven Skiena. Deepwalk: online learning of social representations. In Sofus A. Macskassy, Claudia Perlich, Jure Leskovec, Wei Wang, and Rayid Ghani (eds.), *The 20th ACM SIGKDD International Conference on Knowledge Discovery and Data Mining, KDD '14, New York, NY, USA - August 24 - 27, 2014*, pp. 701–710. ACM, 2014.
- Yu Rong, Wenbing Huang, Tingyang Xu, and Junzhou Huang. Dropedge: Towards deep graph convolutional networks on node classification. In *ICLR*, 2020.
- T. Konstantin Rusch, Michael M. Bronstein, and Siddhartha Mishra. A survey on oversmoothing in graph neural networks. *CoRR*, abs/2303.10993, 2023. doi: 10.48550/arXiv.2303.10993. URL <https://doi.org/10.48550/arXiv.2303.10993>.
- Petar Velickovic, Guillem Cucurull, Arantxa Casanova, Adriana Romero, Pietro Liò, and Yoshua Bengio. Graph attention networks. *CoRR*, abs/1710.10903, 2017.
- Petar Velickovic, Guillem Cucurull, Arantxa Casanova, Adriana Romero, Pietro Liò, and Yoshua Bengio. Graph attention networks. In *ICLR*, 2018.
- Hongwei Wang and Jure Leskovec. Unifying graph convolutional neural networks and label propagation. *CoRR*, 2020.
- Kuansan Wang, Zhihong Shen, Chiyuan Huang, Chieh-Han Wu, Yuxiao Dong, and Anshul Kanakia. Microsoft academic graph: When experts are not enough. *Quantitative Science Studies*, 1(1):396–413, 2020.
- Tongzhou Wang and Phillip Isola. Understanding contrastive representation learning through alignment and uniformity on the hypersphere. In *Proceedings of the 37th International Conference on Machine Learning, ICML 2020, 13-18 July 2020, Virtual Event*, volume 119 of *Proceedings of Machine Learning Research*, pp. 9929–9939. PMLR, 2020.
- Keyulu Xu, Chengtao Li, Yonglong Tian, Tomohiro Sonobe, Ken-ichi Kawarabayashi, and Stefanie Jegelka. Representation learning on graphs with jumping knowledge networks. In Jennifer G. Dy and Andreas Krause (eds.), *Proceedings of the 35th International Conference on Machine Learning, ICML 2018, Stockholmsmässan, Stockholm, Sweden, July 10-15, 2018*, volume 80 of *Proceedings of Machine Learning Research*, pp. 5449–5458. PMLR, 2018.
- Keyulu Xu, Weihua Hu, Jure Leskovec, and Stefanie Jegelka. How powerful are graph neural networks? In *ICLR*, 2019.
- Lingxiao Zhao and Leman Akoglu. Pairnorm: Tackling oversmoothing in gnns. In *ICLR*, 2020.
- Kaixiong Zhou, Xiao Huang, Yuening Li, Daochen Zha, Rui Chen, and Xia Hu. Towards deeper graph neural networks with differentiable group normalization. In *NeurIPS*, 2020.
- Kaixiong Zhou, Xiao Huang, Daochen Zha, Rui Chen, Li Li, Soo-Hyun Choi, and Xia Hu. Dirichlet energy constrained learning for deep graph neural networks. In *Advances in Neural Information Processing Systems 34: Annual Conference on Neural Information Processing Systems 2021, NeurIPS 2021, December 6-14, 2021, virtual*, pp. 21834–21846, 2021.

Hao Zhu, Ke Sun, and Peter Koniusz. Contrastive laplacian eigenmaps. *Advances in Neural Information Processing Systems*, 34:5682–5695, 2021.

A Similarity between Oversmoothing and Dimensional Collapse

In (Rusch et al., 2023), the authors describe *oversmoothing* as a phenomenon that the node representation vectors are indistinguishable from each other and thus deteriorate the performance of downstream tasks. Inspired by this, we could measure the magnitude of graph oversmoothing by the metric of covariance mean as follows:

$$\begin{aligned} \text{covariance}(h) &= \frac{1}{n} \sum_i (h_i - \bar{h})(h_i - \bar{h}) \\ \bar{h} &= \frac{1}{n} \sum_i h_i \end{aligned}$$

where h_i is the node representation for node i and $\text{covariance}(h) = 0$ indicates that the learned representation is indistinguishable and the deep model suffers from an oversmoothing issue. Notice that the dimensional collapse is observed when the covariance matrix of the node representations is not full-rank (i.e., the number of non-zero singular values is less than the dimension of the node representation in Figure 1). When $\text{covariance}(h) = 0$, it also indicates that $h_i = h_j = \bar{h}$ for all i and j , and the rank of the covariance matrix of the node representation matrix is 0 (While a large value of $\text{covariance}(h)$ does not mean that the performance is). In other words, the graph model suffers from complete collapse, where all node representations shrink to a single point. Thus, we could see that the oversmoothing issue is highly related to dimensional collapse.

B Visualization of the Weight of Each Layer With Different Weighting Functions

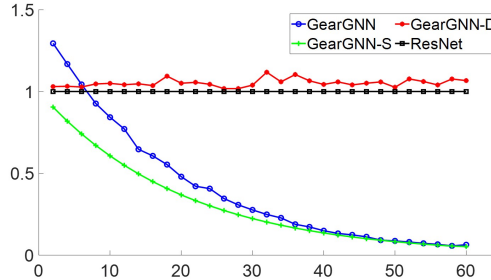


Figure 7: Weight Visualization. The y -axis represents the weight of each layer, and the x -axis represents the index of each layer, in deeper models.

Here, we visualize the weight of each layer with different weighting functions on the Cora dataset. In this experiment, we fix the feature dimension of the hidden layer to be 50; the total iteration is set to be 3000; the number of layers is set to be 60; the sampling batch size for GearGNN is 10; GCN is chosen as the backbone model; λ is set to be 20. In Figure 7, The x -axis is the index of each layer, and the y -axis is the weight for each layer. GearGNN-S removes the similarity measurement $e^{\cos(\mathbf{H}^{(1)}, \tilde{\mathbf{H}}^{(l)})}$ in Eq. 5 and GearGNN-D removes the decaying weight factor and only keeps the exponential cosine similarity $e^{\cos(\mathbf{H}^{(1)}, \tilde{\mathbf{H}}^{(l)})}$ to measure the weight for each layer. GearGNN-S achieves the simplified WG-ResNet in GearGNN, which removes the exponential cosine similarity $e^{\cos(\mathbf{H}^{(1)}, \tilde{\mathbf{H}}^{(l)})}$ in GearGNN. By observation, we find that (1) ResNet sets the weight of each layer to be 1, which easily leads to *shading neighbors* effect when stacking more layers, because the faraway neighbor information becomes more dominant in the GCN information aggregation; (2) without weight decaying factor, the weight for each layer in GearGNN-D fluctuates because they are randomly independent. More specially, the weights for the last several layers (e.g., $L=58$ or $L=60$) are larger than the weights for the first several layers, which contradicts the intuition that the first several layers should be more important than the last several layers; (3) the weights for each layer in both GearGNN and GearGNN-S reduce as the number of layers increase, which suggests that both of them could address the *shading neighbors* effect to some extents; (4) combining the results from Table 4, GearGNN achieves better performance than

GearGNN-S, as it imposes larger weights to the first several layers, which verifies that the learnable similarity $\text{sim}(\mathbf{H}^{(1)}, \tilde{\mathbf{H}}^{(l)})$ achieves better performance with the enlarged hypothesis space for neural networks.

C Proof for Lemma 2.1

Lemma 2.1: \mathcal{L}_{SCL} is a generative adversarial network (GAN) based contrastive learning loss, which could be written as follows:

$$\min_{\theta} \mathcal{L}_{\text{SCL}} = \max_{\theta} \int_e (\tilde{p}_p(e) \log(D(e)) + \tilde{p}_n(e) \log(1 - D(e))) de$$

where $D(e) = f(\mathbf{z}_i, \mathbf{z}_j)$ is the discriminator of GAN with $e = (v_i, v_j)$, $\tilde{p}_p(e) = \sigma p_p(e)$ and $\tilde{p}_n(e) = \gamma p_n(e)$.

Proof. Since $D(e) = f(\mathbf{z}_i, \mathbf{z}_j)$, we have

$$\begin{aligned} \min_{\theta} \mathcal{L}_{\text{SCL}} &= -\mathbb{E}_{v_i \sim V} [\mathbb{E}_{v_j \in \mathcal{N}_i} (\sigma_{ij} \log(f(\mathbf{z}_i, \mathbf{z}_j))) + \mathbb{E}_{v_k \in \bar{\mathcal{N}}_i} (\gamma_{ik} \log(1 - f(\mathbf{z}_i, \mathbf{z}_k)))] \\ &= -\min_{\theta} \int_e (p_p(e) \sigma \log(D(e)) + (p_n(e) \gamma) \log(1 - D(e))) de \\ &= \max_{\theta} \int_e (\tilde{p}_p(e) \log(D(e)) + \tilde{p}_n(e) \log(1 - D(e))) de \end{aligned}$$

□

D Reproducibility

All of the real-world datasets are publicly available. The experiments are performed on a Windows machine with a 16GB RTX 5000 GPU. The code of our algorithm is in an anonymous link ¹. We provide the detailed experimental setting for each experiment shown in Table 6.

Table 6: Hyperparameters for GearGNN shown in Table 2.

| Method | GearGNN |
|----------|-------------------------------|
| Cora | $\lambda = 20, \alpha = 0.03$ |
| CiteSeer | $\lambda = 10, \alpha = 0.02$ |
| PubMed | $\lambda = 18, \alpha = 0.1$ |
| Reddit | $\lambda = 20, \alpha = 0.02$ |

Moreover, we set the learning rate to be 0.001 and the optimizer is RMSProp, which is one variant of ADAGRAD (Duchi et al., 2011).

E Additional Effectiveness Analysis

We conduct the additional experiments by comparing our proposed method with RevGCN-Deep (Li et al., 2021) and EGNN (Zhou et al., 2021). We set the number of layers for all baseline methods to 60 for Cora, Citeseer, PubMed, and Reddit. For the OGB-arXiv dataset, we set the number of layers to 10 for all methods.

Table 7: Additional Node Classification Comparison.

| Method | Cora ($L=60$) | CiteSeer ($L=60$) | PubMed ($L=60$) | Reddit ($L=60$) | OGB-arXiv ($L=10$) |
|-------------|---------------------|---------------------|---------------------|---------------------|----------------------|
| RevGCN-Deep | 0.7458 ± 0.0084 | 0.5137 ± 0.0099 | 0.8139 ± 0.0015 | 0.8853 ± 0.0383 | 0.7354 ± 0.0009 |
| EGNN | 0.7961 ± 0.0036 | 0.6566 ± 0.0060 | 0.8138 ± 0.0026 | 0.8772 ± 0.0040 | 0.7247 ± 0.0015 |
| GearGNN | 0.8059 ± 0.0028 | 0.6655 ± 0.0117 | 0.8185 ± 0.0016 | 0.9721 ± 0.0011 | 0.7401 ± 0.0009 |

¹<https://drive.google.com/file/d/1cbNI74lhTb3Ls0KhgVHT1btNz20ZLb60/view?usp=sharing>

F Additional Hyperparameter Analysis

Here, we conduct additional hyperparameter analysis of GearGNN, i.e., α in the overall loss function of Eq 1.

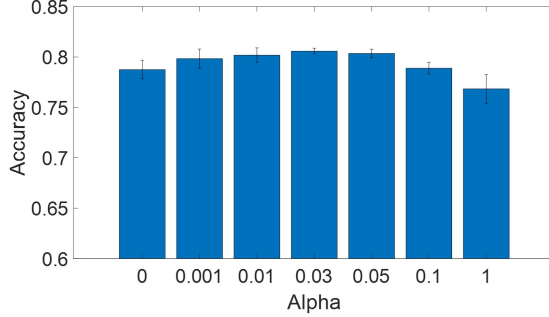


Figure 8: Hyperparameter Analysis, i.e., α vs Node Classification Accuracy.

To analyze the hyperparameter α in GearGNN, we fix the feature dimension of the hidden layer to be 50, the total iteration is set to be 3000, the number of layers is set to be 60, the sampling batch size for GearGNN is 10, GCN is chosen as the backbone model, and the dataset is Cora. We gradually increase the value of α and record the accuracy. The experiment is repeated five times in each setting. In Figure 8, the x-axis is α and the y-axis is the accuracy score. By observation, when $\alpha = 1$, the performance is worst and the performance begins to increase by decreasing the value of α . It achieves the best accuracy when $\alpha = 0.03$. The performance starts to decrease again if we further decrease the value of α . Our conjecture is that when α is large, it will dominate the overall objective function, thus jeopardizing the classification performance. Besides, if we set the value of α to be a small number (i.e., $\alpha = 0.001$), the performance also decreases. In addition, comparing with the performance without using SCL regularization (i.e., $\alpha = 0$), our proposed method with $\alpha = 0.03$ can boost the performance by more than 1.8%, which demonstrates that our proposed SCL alleviates the issue of oversmoothing to some extent.

G Efficiency Analysis

Here, we conduct an efficiency analysis regarding our proposed method in the Cora dataset. We fix the feature dimension of the hidden layer to be 50, the total iteration is set to be 1500, the sampling batch size for GearGNN and GearGNN-S is 10, and GCN is chosen as the backbone model. We gradually increase the number of layers and record the running time.

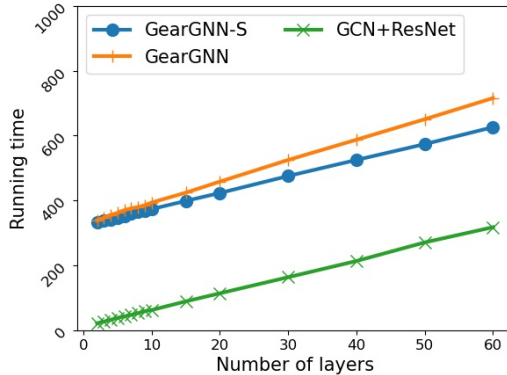


Figure 9: The Number of Layers vs Running Time (in seconds) on Cora.

In Figure 9, the x -axis is the number of layers and the y -axis is the running time in seconds. We observe that the running time of both GearGNN and GearGNN-S is linearly proportional to the number of layers. Comparing the running time of GearGNN, the running time of GearGNN-S is further reduced after the weighting function in GearGNN (e.g., $\text{sim}(\cdot)$) is replaced by a constant.

H Sampling Method for SCL

To realize SCL expressed in Eq. 5, we need to get the positive nodes v_j and negative nodes v_k towards the selected central node v_i . To avoid iterating over all existing nodes or randomly sampling several nodes, we propose to sample positive nodes v_j and negative nodes v_k from the star subgraph S_i of the central node v_i . Moreover, to make the sampling scalable and to reduce the search space of negative nodes, we propose a batch sampling method.

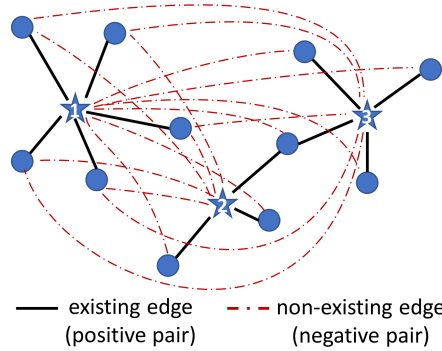


Figure 10: Batch Sampling. Each star node in the figure corresponds to node v_i in Eq. 5.

As shown in Figure 10, the batch size is controlled by the number of central nodes (i.e., star nodes in the figure). For each central node, the positive nodes are those 1-hop neighbors, and the negative nodes consist of unreachable nodes. In our batch sampling, we strictly constrain that the positive nodes are only from the 1-hop neighborhood for the following three reasons: (1) they are efficient to be accessed; (2) considering all k -hop neighbors as positive will enlarge the scope of positive nodes and further decrease the intimacy of the directly connected nodes; (3) 1-hop positive nodes in the star subgraph can preserve enough useful information, compared with the positive nodes from the whole graph. For the third point, we prove it through the *graph influence loss* (Huang & Zitnik, 2020) in Proposition H.1, and the formal definition of *graph influence loss* is given in the following paragraph after Proposition H.1.

Proposition H.1 (Bounded Graph Influence Loss for Sampling Positive Pairs Locally). *Taking GCN as an example of GNN, the graph influence loss $R(v_c)$ on node v_c w.r.t **positive nodes from the whole graph** against **positive nodes from the 1-hop neighborhood star subgraph** is bounded by $R(v_c) \leq (n - d_c) \frac{\mu}{(D_{GM}^{\mathcal{P}_*})^{|\mathcal{P}_*|}}$, where n is the number of nodes, d_c is the degree of node v_c including the self-loop, μ is a constant, \mathcal{P}_* is the path from center node v_c to a 1-hop outside node v_s which has the maximal node influence I_{v_c, v_s} , and $|\mathcal{P}_*|$ denotes the number of nodes in path \mathcal{P}_* .*

Proof. According to the assumption of (Wang & Leskovec, 2020), $\sigma(\cdot)$ can be identity function and $\mathbf{W}^{(\cdot)}$ can be identity matrix. Then, the hidden node representation (of node v_c) in the last layer of GCN can be written as follows.

$$\mathbf{h}_c^{(\infty)} = \frac{1}{D_{c,c}} \sum_{v_i \in \mathcal{N}_c} A_{c,i} \mathbf{h}_i^{(\infty)}$$

Then, based on the above equation, we can iteratively replace $\mathbf{h}_i^{(\infty)}$ with its neighbors until the representation $\mathbf{h}_s^{(\infty)}$ of node v_s is included. The extension procedure is written as follows.

$$\begin{aligned} \mathbf{h}_c^{(\infty)} &= \frac{1}{D_{c,c}} \sum_{v_i \in \mathcal{N}_c} A_{c,i} \frac{1}{D_{i,i}} \sum_{v_j \in \mathcal{N}_i} A_{i,j} \dots \\ &\quad \frac{1}{D_{k,k}} \sum_{v_s \in \mathcal{N}_k} A_{k,s} \mathbf{h}_s^{(\infty)} \end{aligned}$$

The above equation suggests that the influence from the positive node v_s to the center node v_c is through the path $\mathcal{P} = (v_c, v_i, v_j, \dots, v_k, v_s)$.

Following the above path formation and assuming the edge weight $A(i, j)$ as the positive constant, according to (Huang & Zitnik, 2020), we can obtain the node influence I_{v_c, v_s} of v_s on v_c as follows.

$$I_{v_c, v_s} = \|\partial \mathbf{h}_c^{(\infty)} / \partial \mathbf{h}_s^{(\infty)}\| \leq \frac{\mu}{(D_{GM}^{\bar{\mathcal{P}}})^{|\bar{\mathcal{P}}|}}$$

where μ is a constant, $D_{GM}^{\bar{\mathcal{P}}}$ is the geometric mean of the degree of nodes sitting in path $\bar{\mathcal{P}}$, and $\bar{\mathcal{P}}$ is the path from the positive node v_s to the center node v_c that could generate the maximal multiplication of normalized edge weight, $|\bar{\mathcal{P}}|$ denotes the number of nodes in path $\bar{\mathcal{P}}$.

The above analysis suggests that the node influence of positive long-distance nodes is decaying.

Hence, the graph influence loss about learning node v_c from **the whole graph positive nodes** versus **from the 1-hop localized positive nodes** can be expressed as follows.

$$\begin{aligned} I_G(v_c) - I_L(v_c) &= I_{v_c, v_1} + I_{v_c, v_2} + \dots + I_{v_c, v_{n-d_c}} \\ &\leq \sum_{i=1}^{n-d_c} \frac{\mu_i}{(D_{GM}^{\bar{\mathcal{P}}_i})^{|\bar{\mathcal{P}}_i|}} \\ &\leq (n - d_c) \frac{\mu_*}{(D_{GM}^{\bar{\mathcal{P}}_*})^{|\bar{\mathcal{P}}_*|}} \end{aligned}$$

where $I_G(v_c)$ denotes global influence, $I_L(v_c)$ is the influence for star subgraph, d_c is the degree of node v_c (including self-loop), and $\frac{\mu_*}{(D_{GM}^{\bar{\mathcal{P}}_*})^{|\bar{\mathcal{P}}_*|}}$ is the maximal among all $\frac{\mu_i}{(D_{GM}^{\bar{\mathcal{P}}_i})^{|\bar{\mathcal{P}}_i|}}$. \square

Specifically, the graph influence loss (Huang & Zitnik, 2020) $R(v_c)$ can be expressed as $R(v_c) = I_G(v_c) - I_L(v_c)$, which is determined by the global graph influence on v_c (i.e., $I_G(v_c)$) and the star subgraph influence on v_c (i.e., $I_L(v_c)$). Then, to compute the graph influence $I_G(v_c)$, we need to compute the node influence of each node v_j to node v_c , where node v_j is reachable from node v_c . Based on the final output node representation vectors, the node influence is expressed as $I_{v_c, v_j} = \|\partial \mathbf{h}_c^{(\infty)} / \partial \mathbf{h}_j^{(\infty)}\|$, and the norm can be any subordinate norm (Wang & Leskovec, 2020). Then, $I_G(v_c)$ is computed by the $L1$ -norm of the following vector, i.e., $I_G(v_c) = \|[I_{v_c, v_1}, I_{v_c, v_2}, \dots, I_{v_c, v_n}]\|_1$. Similarly, we can compute the star subgraph influence $I_L(v_c)$ on node v_c . The only difference is that we collect each reachable node v_j in the star subgraph L (i.e., 1-hop neighbors of v_c). Overall, in Proposition H.1, we show why positive pairs can be locally sampled with the support from graph influence loss of a node representation vector output by the GCN final layer.